A Letters Journal Exploring the Frontiers of Physics

November 2019

EPL, **128** (2019) 34002
doi: 10.1209/0295-5075/128/34002

www.epljournal.org

# Two exact schemes to realize thermal chameleonlike metashells

S. Yang[(a)], L. J. Xu and J. P. Huang[(b)]

*Department of Physics, State Key Laboratory of Surface Physics, and Key Laboratory of Micro and Nano Photonic Structures (MOE), Fudan University - Shanghai 200438, China*

received 6 October 2019; accepted in final form 17 November 2019
published online 24 January 2020

PACS 44.10.+i – Heat conduction
PACS 05.70.-a – Thermodynamics
PACS 81.05.Zx – New materials: theory, design, and fabrication

**Abstract** – Intelligence has become one of the developing trends of thermal metamaterials in order to meet different practical requirements. By considering the temperature-dependent and specially designed thermal conductivities, chameleonlike behaviors have been revealed to realize adaptive responses to nearby objects. However, the existing schemes are approximately valid only for a small working range of nearby thermal conductivities. This fact limits practical applications. To solve this problem, here we propose two exact schemes to realize thermal chameleonlike behaviors, say, monolayer schemes and bilayer schemes. By carefully designing the thermal conductivities of the metashells, we find that the effective thermal conductivities can exactly change with those of nearby objects. Theoretical derivations are validated by finite-element simulations. We further extend the monolayer schemes to three dimensions. The proposed schemes can work as a type of multifunction materials to meet different requirements of thermal conductivities. This work provides intelligence to thermal conductivities, which may inspire further development of intelligent thermal metamaterials.



**Introduction.** – Thermal metamaterials have made a considerable impact on the field of heat management due to their specially designed structures and conductivities. Some representative examples are thermal cloaks [1–11], thermal transparency [12,13], thermal bending [14–17], thermal camouflage/illusion [18–21], heat rectification [22], etc.

However, these schemes almost exhibit no intelligence, which means that they cannot adapt to the change of nearby objects. Recent work has made some advances in intelligence, and designed chameleonlike metashells in heat conduction [23]. However, the existing results [23] are only approximately valid, which rely merely on a small working range of nearby objects. Furthermore, in ref. [23], the use of both strong anisotropy and near zero thermal conductivity limits the applications as well.

To solve these problems, here we propose two exact schemes for realizing metashells with thermal chameleonlike behavior. Concretely speaking, the designed metashells can always imitate the thermal conductivity of nearby objects, thus yielding an undistorted temperature profile outside the metashell (as if the metashell was the same as the object in the vicinity). Our method depends on the exact derivation of the effective thermal conductivity of core-shell structures. By solving the Laplace equation, we can accurately design the thermal conductivities of the metashells, and our theoretical derivations are validated by finite-element simulations. This kind of metashells have broad application prospects for their adaptive responses. For example, they can act as a type of intelligent materials to satisfy different demands under different conditions. They can also be used to realize intelligent thermal camouflage to mislead infrared detection.

**Theory for thermal chameleonlike metashells.** –

*Anisotropic monolayer schemes.* We discuss the properties of the core-shell structure presented in fig. 1(a). We set the radius and the thermal conductivity of the core to be $r_c$ and $\kappa_c$, and those of the shell to be $r_s$ and $\kappa_s = \mathrm{diag}(\kappa_{rr}, \kappa_{\theta\theta})$ with $\kappa_{\theta\theta}/\kappa_{rr} < 0$ in cylindrical coordinates $(r, \theta)$. The dominant equation in heat conduction is

$$\boldsymbol{\nabla} \cdot (-\kappa \boldsymbol{\nabla} T) = 0, \tag{1}$$

where $\kappa$ and $T$ are the tensorial thermal conductivity and temperature, respectively.

[(a)] E-mail: syang18@fudan.edu.cn
[(b)] E-mail: jphuang@fudan.edu.cn

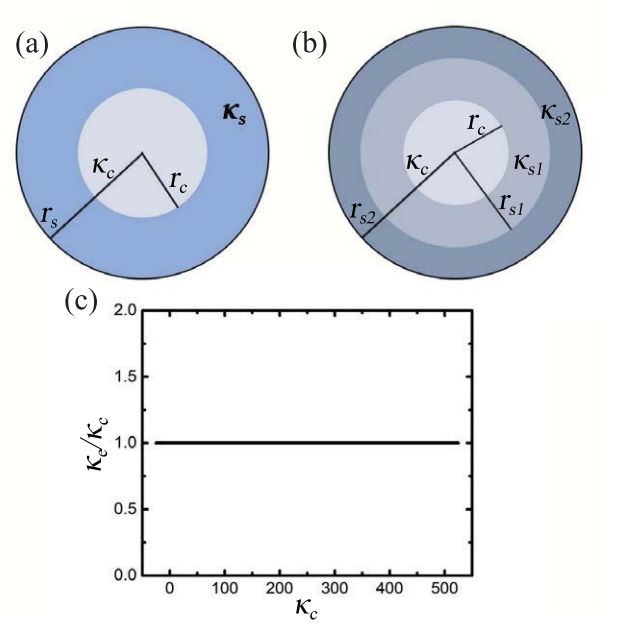


Fig. 1: Schematic diagrams of (a) core-shell structure or (b) core-shell-shell structure in two dimensions. Panel (c) shows the functional relationship between $\kappa_e/\kappa_c$ and $\kappa_c$ when the thermal chameleonlike metashells work.

Equation (1) can be expressed in cylindrical coordinates as

$$\frac{\partial}{\partial r}\left(r\kappa_{rr}\frac{\partial T}{\partial r}\right)+\frac{\partial}{\partial \theta}\left(\kappa_{\theta\theta}\frac{\partial T}{r\partial \theta}\right)=0. \tag{2}$$

The general solution of eq. (2) is

$$\begin{aligned}
&T(\kappa_{\theta\theta}/\kappa_{rr}<0)=A_0+B_0\ln r\\
&+\sum_{i=1}^{\infty}[A_i\sin(i\theta)+B_i\cos(i\theta)]\sin(im\ln r)\\
&+\sum_{i=1}^{\infty}[C_i\sin(i\theta)+D_i\cos(i\theta)]\cos(im\ln r), \qquad (3)\\
&T(\kappa_{\theta\theta}/\kappa_{rr}>0)=E_0+F_0\ln r\\
&+\sum_{i=1}^{\infty}[E_i\sin(i\theta)+F_i\cos(i\theta)]r^{in}\\
&+\sum_{i=1}^{\infty}[G_i\sin(i\theta)+H_i\cos(i\theta)]r^{-in}, \qquad (4)
\end{aligned}$$

where $m=\sqrt{-\kappa_{\theta\theta}/\kappa_{rr}}$, and $n=\sqrt{\kappa_{\theta\theta}/\kappa_{rr}}$.

The temperature distributions of the core ($T_c$), the shell ($T_s$), and the matrix ($T_m$) can then be determined by the following boundary conditions:

$$\begin{cases}
T_c<\infty,\\
T_c(r_c)=T_s(r_c),\\
T_s(r_s)=T_m(r_s),\\
(-\kappa_c\partial T_c/\partial r)_{r_c}=(-\kappa_{rr}\partial T_s/\partial r)_{r_c},\\
(-\kappa_{rr}\partial T_s/\partial r)_{r_s}=(-\kappa_m\partial T_m/\partial r)_{r_s},\\
\boldsymbol{\nabla}T_m(r\to\infty)=\boldsymbol{\nabla}T_0,
\end{cases} \tag{5}$$

where $\boldsymbol{\nabla}T_0$ represents the external uniform potential gradient.

We only require to keep several terms with $i=1$ in eqs. (3) and (4) because of the symmetric boundary conditions of eq. (5):

$$\begin{aligned}
T(\kappa_{\theta\theta}/\kappa_{rr}<0) &= A_0+B_1\cos\theta\sin(m\ln r)\\
&\quad +D_1\cos\theta\cos(m\ln r), \qquad (6)\\
T(\kappa_{\theta\theta}/\kappa_{rr}>0) &= E_0+F_1r^n\cos\theta\\
&\quad +H_1r^{-n}\cos\theta. \qquad (7)
\end{aligned}$$

Therefore, we can obtain $T_m = E_0 + F_1 r\cos\theta + H_1 r^{-1}\cos\theta$ for an isotropic matrix. We set $H_1$ to be zero to ensure the external field undistorted. Then we can derive the effective thermal conductivity of the core-shell structure $\kappa_e$ as

$$\kappa_e=m\kappa_{rr}\frac{\kappa_c+m\kappa_{rr}\tan(m\ln\sqrt{p})}{m\kappa_{rr}-\kappa_c\tan(m\ln\sqrt{p})}, \tag{8}$$

where $m=\sqrt{-\kappa_{\theta\theta}/\kappa_{rr}}$, and $p=(r_c/r_s)^2$ is the core fraction. As defined in this work, thermal chameleonlike metashells are characterized by the adaptive responses to inside objects. Namely, the effective thermal conductivity of the shell ($\kappa_s$) is always equal to that of the inside object,

$$\kappa_s=\kappa_c. \tag{9}$$

Based on the requirement of eq. (9), the effective thermal conductivity of the core-shell structure ($\kappa_e$) must be

$$\kappa_e=\kappa_c. \tag{10}$$

Then, we should find some special relations to make eq. (8) turn into eq. (10). Fortunately, we find one

$$\sqrt{-\kappa_{\theta\theta}/\kappa_{rr}}\ln\sqrt{p}=-N^+\pi, \tag{11}$$

where $N^+(=1,2,3,\ldots)$ can be any positive integer. Clearly, the requirement of eq. (10) is strictly satisfied with eq. (11).

*Isotropic bilayer schemes.* We also discuss the properties of the core-shell-shell structure presented in fig. 1(b). We set the core with radius $r_c$ and thermal conductivity $\kappa_c$, and the two shells with radius $r_{s1}$ and $r_{s2}$, and thermal conductivities $\kappa_{s1}$ and $\kappa_{s2}$, respectively. The effective thermal conductivity of the core-shell-shell structure $\kappa_e$ can be expressed as

$$\kappa_e=\kappa_{s2}\frac{\kappa_{12}+\kappa_{s2}+(\kappa_{12}-\kappa_{s2})p_{12}}{\kappa_{12}+\kappa_{s2}-(\kappa_{12}-\kappa_{s2})p_{12}}, \tag{12}$$

where $p_{12} = (r_{s1}/r_{s2})^2$. $\kappa_{12}$ is the effective thermal conductivity of the core plus the first shell, which can be calculated by

$$\kappa_{12} = \kappa_{s1}\frac{\kappa_c + \kappa_{s1} + (\kappa_c - \kappa_{s1})p_c}{\kappa_c + \kappa_{s1} - (\kappa_c - \kappa_{s1})p_c}, \tag{13}$$

where $p_c = (r_c/r_{s1})^2$. We also find a special relation to make eq. (12) turn into eq. (10):

$$(\kappa_{s1} + \kappa_{s2})^2 + (p_c - p_{12})^2 = 0. \tag{14}$$

which gives that $\kappa_{s1} + \kappa_{s2} = 0$ and $p_c - p_{12} = 0$ should be simultaneously satisfied. Clearly, the requirement of eq. (10) is strictly satisfied with eq. (14).

So far, we have theoretically analyzed the thermal chameleonlike metashells in two dimensions, say eq. (11) for monolayer schemes and eq. (14) for bilayer schemes. The presence of thermal chameleonlike metashells can ensure that the effective thermal conductivity of the whole structure corresponds with the core, see fig. 1(c).

*Three-dimensional counterpart of anisotropic monolayer schemes.* The theory for two-dimensional anisotropic monolayer schemes can be extended to three-dimensional schemes. Equation (1) in spherical coordinates is expressed as

$$\frac{1}{r}\frac{\partial}{\partial r}\left(r^2\kappa_{rr}\frac{\partial T}{\partial r}\right) + \frac{1}{\sin\theta}\frac{\partial}{\partial\theta}\left(\sin\theta\kappa_{\theta\theta}\frac{\partial T}{r\partial\theta}\right) = 0. \tag{15}$$

The general solution of eq. (15) is

$$\begin{aligned}
&T(\kappa_{\theta\theta}/\kappa_{rr} < -1/8) = A_0 + B_0 r^{-1} \\
&+\sum_{i=1}^{\infty} r^{-1/2}[A_i \sin(s\ln r) + B_i\cos(s\ln r)] \\
&\times P_i(\cos\theta), \qquad (16)\\
&T(-1/8 < \kappa_{\theta\theta}/\kappa_{rr} < 0) = C_0 + D_0 r^{-1} \\
&+\sum_{i=1}^{j}(C_i r^{t_1} + D_i r^{t_2})P_i(\cos\theta) \\
&+\sum_{i=j+1}^{\infty} r^{-1/2}[E_i\sin(s\ln r) + F_i\cos(s\ln r)] \\
&\times P_i(\cos\theta), \qquad (17)\\
&T(0 \le \kappa_{\theta\theta}/\kappa_{rr}) = \sum_{i=0}^{\infty}(G_i r^{t_1} + H_i r^{t_2}) \\
&\times P_i(\cos\theta), \qquad (18)
\end{aligned}$$

where $s = \sqrt{-1/4 - i(i+1)\kappa_{\theta\theta}/\kappa_{rr}}$, $t_{1,2} = -1/2 \pm \sqrt{1/4 + i(i+1)\kappa_{\theta\theta}/\kappa_{rr}}$, $i$ is the summation index, $j = \mathrm{INT}[-1/2 + \sqrt{1/4 - \kappa_{rr}/(4\kappa_{\theta\theta})}]$, and $\mathrm{INT}[\cdots]$ is the integral function with respect to .... $P_i$ indicates Legendre polynomials.

In fact, eqs. (17) and (18) turn to be the same with similar boundary conditions to eq. (5) because we only require to keep several terms of $i = 1$. Thus, eqs. (16)–(18) can be simplified as

$$\begin{aligned}
&T(\kappa_{\theta\theta}/\kappa_{rr} < -1/8) = A_0 \\
&+r^{-1/2}[A_1\sin(u\ln r) + B_1\cos(u\ln r)]\cos\theta, \qquad (19)\\
&T(\kappa_{\theta\theta}/\kappa_{rr} > -1/8) = G_0 \\
&+(G_1 r^{v_1} + H_1 r^{v_2})\cos\theta, \qquad (20)
\end{aligned}$$

where $u = \sqrt{-1/4 - 2\kappa_{\theta\theta}/\kappa_{rr}}$, and $v_{1,2} = -1/2 \pm \sqrt{1/4 + 2\kappa_{\theta\theta}/\kappa_{rr}}$,

We set the core with radius $r_c$ and scalar thermal conductivity $\kappa_c$, and the shell with radius $r_s$ and tensorial thermal conductivity $\kappa_s = \mathrm{diag}(\kappa_{rr}, \kappa_{\theta\theta}, \kappa_{\varphi\varphi})$ with $\kappa_{\theta\theta} = \kappa_{\varphi\varphi}$ for brevity. It should be noted that $\kappa_{\theta\theta}/\kappa_{rr} < -1/8$.

We can obtain $T_m = G_0 + (G_1 r + H_1 r^{-2})\cos\theta$ for an isotropic matrix. We set $H_1$ to be zero to ensure the external field undistorted. Then we can derive the effective thermal conductivity of the core-shell structure $\kappa_e$ in three dimensions as

$$\kappa_e = \kappa_{rr}\frac{4u\kappa_c + [2\kappa_c + (1+4u^2)\kappa_{rr}]\tan(u\ln\sqrt[3]{p})}{4u\kappa_{rr} - 2(2\kappa_c + \kappa_{rr})\tan(u\ln\sqrt[3]{p})}, \tag{21}$$

where $p = (r_c/r_s)^3$ is the core fraction.

We also find a special relation to make eq. (21) to satisfy the requirement of eq. (10)

$$\sqrt{-1/4 - 2\kappa_{\theta\theta}/\kappa_{rr}}\ln\sqrt[3]{p} = -N^+\pi, \tag{22}$$

where $N^+(= 1, 2, 3, \cdots)$ can be any positive integer. Clearly, with eq. (22), the requirement of eq. (10) is perfectly satisfied. Therefore, thermal chameleonlike metshells can be achieved in three dimensions with an anisotropic monolayer scheme.

*Explanation for the failure of isotropic bilayer schemes in three dimensions.* Then we consider the isotropic bilayer schemes in three dimensions. We set the core to have radius $r_c$ and scalar thermal conductivity $\kappa_c$, and the two shells to have radii $r_{s1}$ and $r_{s2}$ and scalar thermal conductivities $\kappa_{s1}$ and $\kappa_{s2}$. Then we can derive the effective thermal conductivity of the core-shell-shell structure $\kappa_e$ as

$$\kappa_e = \kappa_{s2}\frac{\kappa_{12} + 2\kappa_{s2} + 2(\kappa_{12} - \kappa_{s2})p_{12}}{\kappa_{12} + 2\kappa_{s2} - (\kappa_{12} - \kappa_{s2})p_{12}}, \tag{23}$$

where $p_{12} = (r_{s1}/r_{s2})^3$. $\kappa_{12}$ is the effective thermal conductivity of the core plus the first shell, which can be calculated as

$$\kappa_{12} = \kappa_{s1}\frac{\kappa_c + 2\kappa_{s1} + 2(\kappa_c - \kappa_{s1})p_c}{\kappa_c + 2\kappa_{s1} - (\kappa_c - \kappa_{s1})p_c}, \tag{24}$$

where $p_c = (r_c/r_{s1})^3$.

Although we find a special relation to make eq. (23) turn into eq. (10),

$$\begin{aligned}
&[(p_{12} - 2p_c + p_c p_{12})\kappa_c - (p_c - 2p_{12} + p_c p_{12})\kappa_{s1}]^2 \\
&+(\kappa_{s1} + 2\kappa_{s2})^2 = 0, \qquad (25)
\end{aligned}$$

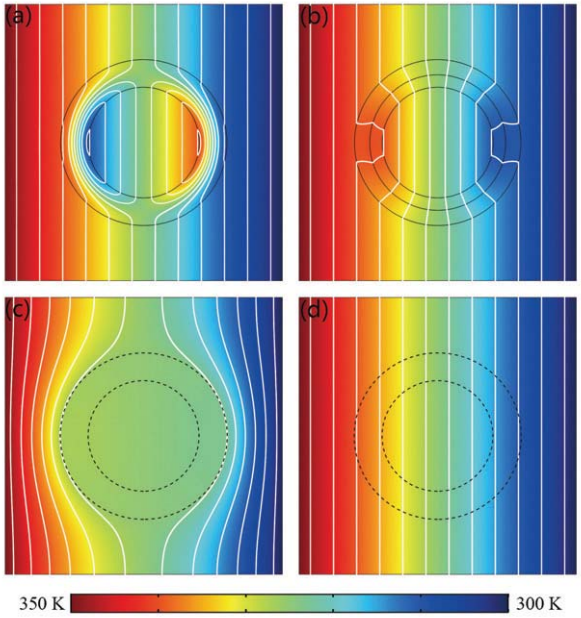


Fig. 2: The simulation box is $10 \times 10\,\mathrm{cm}^2$. The inner and outer radii in (a), (c), and (d) are 2 and 3 cm. The three radius in (b) are 2, $\sqrt{6}$, and 3 cm. The thermal conductivities of the thermal chameleonlike metashells are $\kappa_s = \mathrm{diag}(10, -600.33)\,\mathrm{Wm^{-1}K^{-1}}$ in (a), $-10\,\mathrm{Wm^{-1}K^{-1}}$ for the inner shell and 10 for the outer shell in (b). The thermal conductivity of the normal shell is $5\,\mathrm{Wm^{-1}K^{-1}}$ in (c) throughout this work. The thermal conductivity of the reference shell is the same as the background for (d). The thermal conductivities of the inside core and outside background are $0.1\,\mathrm{Wm^{-1}K^{-1}}$.

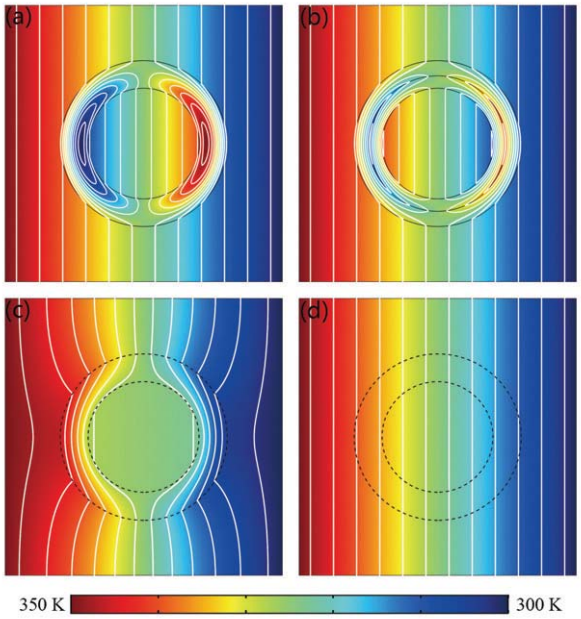


Fig. 3: All the parameters are the same as those for fig. 2 except for the thermal conductivities of the inside core and outside background, say $100\,\mathrm{Wm^{-1}K^{-1}}$.

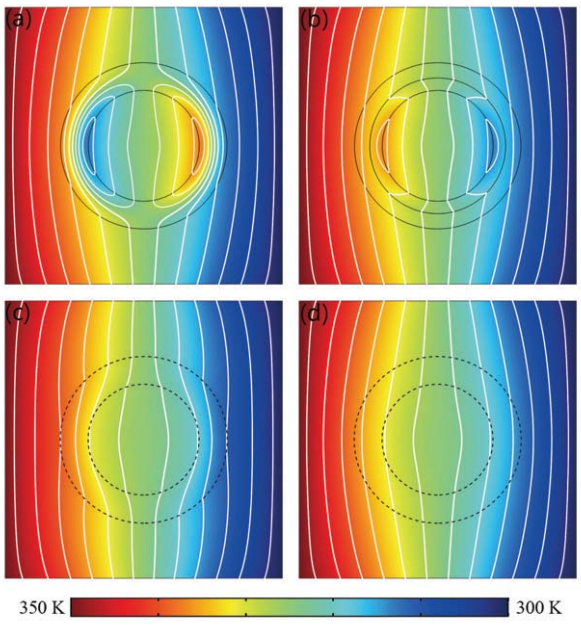


Fig. 4: All the parameters are the same as those for fig. 2 except for the thermal conductivities of the inside core and outside background, say $\mathrm{diag}(10, 20)\,\mathrm{Wm^{-1}K^{-1}}$.

Equation (25) is dependent on $\kappa_c$. This means that the chameleonlike behavior is dependent on the core property, which is not what we expect. Therefore, isotropic bilayer schemes fail in three dimensions.

**Simulations of thermal chameleonlike metashells.** – We perform finite-element simulations to validate the two proposed schemes with COMSOL Multiphysics [24]. To perform simulations, we set the thermal conductivities of the inside core and outside background to be the same. Then, we compare the results of thermal chameleonlike metashells (figs. 2(a), (b)), a normal shell (fig. 2(c)), and a reference shell (fig. 2(d)). Clearly, the same temperature profiles are obtained outside the thermal chameleonlike metashells (figs. 2(a), (b)) and the reference shell (fig. 2(d)). Thus, thermal chameleonlike metashells do adaptively change their effective thermal conductivity according the nearby changes as expected. In contrast, the different background thermal profiles between the normal shell (fig. 2(c)) and the reference shell (fig. 2(d)) show that a normal shell does not possess the ability to change adaptively.

To validate the robustness, we change the thermal conductivities of the inside core and outside background, and keep those of the thermal chameleonlike metashells unchanged, to create a different condition; see fig. 3. As expected, thermal chameleonlike metashells change their effective thermal conductivities adaptively according to the nearby changes. As a result, the temperature distributions outside the chameleonlike metashells (figs. 3(a), (b)) and the reference shell (fig. 3(d)) are the same. However,

that outside the normal shell (fig. 3(c)) is different, which exhibits no adaptivity.

Finally, we consider an anisotropic case to show the capability of the thermal chameleonlike metashells. Similarly, we keep the thermal chameleonlike metashells unchanged, and change the thermal conductivities of the inside core and outside background to be anisotropic; see fig. 4. The same conclusion can be obtained from the same background temperature distributions between figs. 4(a)–(d). Certainly, the normal shell fails again (fig. 4(c)).

**Discussion and conclusion.** – We have proposed and confirmed the performance of two kinds of thermal chameleonlike metashells by both theoretical analyses and finite-element simulations. Our results have shown that the two schemes are exactly valid, indicating that they can work for various changes of nearby objects. Anisotropic monolayer schemes can be applied to both two-dimensional and three-dimensional cases, while isotropic bilayer schemes can be extended to three-dimensional cases. However, if we fabricate the quasi–two-dimensional samples, isotropic bilayer schemes are more useful because the isotropic parameters are easier to achieve compared with the positive and negative anisotropic tensors. For experimental realization, we suggest that readers may use layered structures and external heat or hold sources to design the samples. They are both powerful tools in the course of the experiment although one positive and one negative anisotropic tensors are difficult to match.

In this work, apparent negative thermal conductivities [25] have been applied in our design. Although they do not occur in nature according to the second law of thermodynamics, they can be artificially realized by adding extra heat energy [26–28]. Apparently negative thermal conductivities mean that the direction of the heat flux is from low temperature to high temperature. It is just a macro phenomenon rather than an inherent mechanism, and hence the second law of thermal dynamics is not violated. To make it possible, we manually give a local high (or low) temperature to achieve the same phenomena. Particularly, in fig. 5 and fig. 6 of ref. [27], Yang *et al.* show the theoretial/simulation and experimental method for achieving the apparent negative thermal conductivity, respectively. Meanwhile, fig. 5 of ref. [28] shows a careful design of apparent negative thermal conductivity by using real line heat sources or point heat sources. In this sense, the two schemes proposed in this work have practical significance.

In summary, we have presented two exact schemes to realize thermal adaptive responses to the changing objects in the vicinity. Such schemes can work as multifunction materials to meet various requirements of thermal conductivities under different conditions. This work also provides guidance to other diffusive fields.

* * *

We acknowledge the financial support by the National Natural Science Foundation of China under Grant No. 11725521.

REFERENCES

[1] Fan C. Z., Gao Y. and Huang J. P., *Appl. Phys. Lett.*, **92** (2008) 251907.
[2] Chen T. Y., Weng C.-N. and Chen J.-S., *Appl. Phys. Lett.*, **93** (2008) 114103.
[3] Narayana S. and Sato Y., *Phys. Rev. Lett.*, **108** (2012) 214303.
[4] Xu H. Y., Shi X. H., Gao F., Sun H. D. and Zhang B. L., *Phys. Rev. Lett.*, **112** (2014) 054301.
[5] Han T. C., Bai X., Gao D. L., Thong J. T. L., Li B. W. and Qiu C. W., *Phys. Rev. Lett.*, **112** (2014) 054302.
[6] Ma Y. G., Liu Y. C., Raza M., Wang Y. D. and He S. L., *Phys. Rev. Lett.*, **113** (2014) 205501.
[7] Shen X. Y. and Huang J. P., *Int. J. Heat Mass Transfer*, **78** (2014) 1.
[8] Hu R., Xie B., Hu J. Y., Chen Q. and Luo X. B., *EPL*, **111** (2015) 54003.
[9] Shen X. Y., Li Y., Jiang C. R., Ni Y. S. and Huang J. P., *Appl. Phys. Lett.*, **109** (2016) 031907.
[10] Li Y., Zhu K. J., Peng Y. G., Li W., Yang T. Z., Xu H. X., Chen H., Zhu X. F., Fan S. H. and Qiu C. W., *Nat. Mater.*, **18** (2019) 48.
[11] Han T. C., Yang P., Li Y., Lei D. Y., Li B. W., Hippalgaonkar K. and Qiu C. W., *Adv. Mater.*, **30** (2018) 1804019.
[12] He X. and Wu L. Z., *Phys. Rev. E*, **88** (2013) 033201.
[13] Yang T. Z., Bai X., Gao D. L., Wu L. Z., Li B. W., Thong J. T. L. and Qiu C. W., *Adv. Mater.*, **27** (2015) 7752.
[14] Vemuri K. P. and Bandaru P. R., *Appl. Phys. Lett.*, **104** (2014) 083901.
[15] Yang T. Z., Vemuri K. P. and Bandaru P. R., *Appl. Phys. Lett.*, **105** (2014) 083908.
[16] Xu G. Q., Zhang H. C., Jin Y., Li S. and Li Y., *Opt. Express*, **25** (2017) A419.
[17] Li J. X., Li Y., Li T. L., Wang W. Y., Li L. Q. and Qiu C. W., *Phys. Rev. Appl.*, **11** (2019) 044021.
[18] Han T. C., Bai X., Thong J. T. L., Li B. W. and Qiu C. W., *Adv. Mater.*, **26** (2014) 1731.
[19] Hu R., Zhou S. L., Li Y., Lei D. Y., Luo X. B. and Qiu C. W., *Adv. Mater.*, **30** (2018) 1707237.
[20] Li Y., Bai X., Yang T. Z., Luo H. and Qiu C. W., *Nat. Commun.*, **9** (2018) 273.
[21] Xu L. J. and Huang J. P., *Phys. Lett. A*, **382** (2018) 3313.
[22] Pons M., Cui Y. Y., Ruschhaupt A., Simon M. A. and Muga J. G., *EPL*, **119** (2017) 64001.
[23] Xu L. J., Yang S. and Huang J. P., *Phys. Rev. Appl.*, **11** (2019) 054071.
[24] `http://www.comsol.com/`.
[25] Gao Y. and Huang J. P., *EPL*, **104** (2013) 44001.
[26] Wegener M., *Science*, **342** (2013) 939.
[27] Yang S., Xu L. J. and Huang J. P., *EPL*, **126** (2019) 54001.
[28] Yang S., Xu L. J. and Huang J. P., *Phys. Rev. E*, **99** (2019) 042144.